HHS Public Access

Author manuscript

Biochim Biophys Acta. Author manuscript; available in PMC 2019 September 01.

Published in final edited form as:

Biochim Biophys Acta. 2018 September ; 1864(9 Pt B): 2845–2858. doi:10.1016/j.bbadis.2018.05.016.

Benzodiazepine-refractory status epilepticus, neuroinflammation, and interneuron neurodegeneration after acute organophosphate intoxication

Ramkumar Kuruba, **Xin Wu**, and **Doodipala Samba Reddy***

Department of Neuroscience and Experimental Therapeutics, Texas A&M University Health Science Center, College of Medicine, Bryan, TX 77807

Abstract

Nerve agents and some pesticides such as diisopropylfluorophosphate (DFP) cause neurotoxic manifestations that include seizures and status epilepticus (SE), which are potentially lethal and carry long-term neurological morbidity. Current antidotes for OP intoxication include atropine, 2-PAM and diazepam (a benzodiazepine for treating seizures and SE). There is some evidence for partial or complete loss of diazepam anticonvulsant efficacy when given 30 min later after exposure to an OP; this condition is known as refractory SE. Effective therapies for OP-induced SE are lacking and it is unclear why current therapies do not work. In this study, we investigated the time-dependent efficacy of diazepam in the nerve agent surrogate DFP model of OP intoxication on seizure suppression and neuroprotection in rats, following an early and late therapy. Diazepam (5 mg/kg, IM) controlled seizures when given 10 min after DFP exposure ("early"), but it was completely ineffective at 60 or 120 min ("late") after DFP. DFP-induced neuronal injury, neuroinflammation, and neurodegeneration of principal cells and GABAergic interneurons were significantly reduced by early but not late therapy. These findings demonstrate that diazepam failed to control seizures, SE and neuronal injury when given 60 min or later after DFP exposure, confirming the benzodiazepine refractory SE and brain damage after OP intoxication. In addition, this study indicates that degeneration of inhibitory interneurons and inflammatory glial activation are potential mechanisms underlying these morbid outcomes of OP intoxication. Therefore, novel anticonvulsant antidotes, superior to benzodiazepines, are desperately needed for controlling nerve agent-induced SE and brain injury.

***Correspondence to:** D. Samba Reddy, Ph.D., R.Ph, FAAPS, FAAAS, FAES, Professor & NIH CounterACT Investigator, Department of Neuroscience and Experimental Therapeutics, College of Medicine, Texas A&M University Health Science Center, MREB Bldg 2008, 8447 Riverside Parkway, Bryan, TX 77807, USA, Phone: 979-436-0324, reddy@medicine.tamhsc.edu.

Authorship contributions

All authors participated in research design, running experiments, data analysis and wrote or contributed to the writing of this manuscript and approved it for publication.

Conflict of interest statement

The author declares that the research was conducted in the absence of any commercial or financial relationships that could be construed as a potential conflict of interest.

Keywords

Diazepam; organophosphate; DFP; neuroinflammation; nerve agent; status epilepticus

1. Introduction

Organophosphate (OP) chemicals such as pesticides [parathion, paraoxon and diisopropylfluorophosphate (DFP)] and nerve agents (soman, sarin and VX) are extremely lethal neurotoxic agents [1–5]. These agents act by irreversible inhibition of acetylcholinesterase (AChE), the enzyme that hydrolyzes the excitatory neurotransmitter acetylcholine in the central and peripheral nervous systems [4]. Neurotoxic manifestations following OP exposure includes hypersecretion, miosis, tremors, respiratory distress and convulsions leading to status epilepticus (SE) [5–8]. OP induced SE can last several hours, causing profound brain damage resulting in long-term neuronal dysfunction or death [6–8]. Irreparable neuronal damage, which occurs by SE-related excitotoxicity and other neurotoxic mechanisms of OP intoxication, produces chronic morbidity including the risk of neurological and cognitive deficits [6–9]. The current standard-of-care for OP intoxication includes a three drug regimen: (i) atropine, a muscarinic receptor antagonist; (ii) pralidoxime, an AChE reactivator; and (iii) diazepam, a benzodiazepine anticonvulsant. Effective control of seizures is critical for improved neuroprotection and survival in cases of OP chemical attacks or accidental exposure [2,8].

Diazepam is the standard-of-care for the treatment of seizures and SE caused by exposure from nerve agents or OP pesticides [10–13]. However, there is emerging evidence that there can be partial or complete resistance of seizures or SE to diazepam [14–16]. The refractory SE that occurs following OP poisoning can become self-sustaining and thereby cause significant morbidity and mortality [17]. Earlier studies have suggested that diazepam administered after 30 min post-exposure to either the OP chemical or seizure onset, is ineffective in suppressing seizures and leads to progressive neurologic damage in pilocarpine [18–23] and nerve agent models [14,15]. A progressive, time-dependent loss in the anticonvulsant efficacy of diazepam is clearly evident in the soman model [14]. Moreover, lack of responsiveness to diazepam is confirmed in both paraoxon and DFP models of OP intoxication [24], and with other benzodiazepines such as midazolam [25].

There is a narrow timeline for treatment of seizures in the scenario of a nerve agent attack. There are only 10–30 minutes before irreversible changes occur and this is an unrealistic amount of time for medical intervention in an emergency or mass casualty scenario. The repeated high doses of diazepam that are needed to control seizures or seizure recurrence may result in strong sedation, respiratory depression and mortality. Therapies for nerve agent-induced seizures that are effective after a delayed treatment window (i.e., +30 min post-exposure) are lacking.

In this study, we characterized the time-dependent efficacy of the benzodiazepine diazepam on DFP-induced seizures, SE, and brain injury in rats following an early (10 min) and late (60 or 120 min) post-exposure therapy. Our results demonstrate that delayed therapy with diazepam failed to control SE and neuronal damage, confirming diazepam refractoriness to

DFP-induced SE and brain damage. Massive inhibitory interneuron neurodegeneration and inflammatory glial activation appear as the potential mechanisms underlying these devastating outcomes of OP intoxication.

2. Materials and Methods

2.1. Animals

Male adult Sprague-Dawley rats (250–300 g; Taconic Farms, Rockville, MD) were housed in an environmentally controlled animal facility with a 12 h light-dark cycle. Animals were utilized for experiments after 1 week of acclimatization to the vivarium. Animal care was provided in accordance with the guidelines outlined in the *National Institutes of Health Guide for the Care and Use of Laboratory Animals*. All animal procedures were performed according to a protocol approved by the Institutional Animal Care and Use Committee.

2.2. Experimental design and outcome analysis

The overall experimental protocol is illustrated in Fig. 1. We sought to rigorously test the time-course efficacy of diazepam in the DFP model (rat oral LD_{50} 5 mg/kg), a commonly used OP pesticide that has been considered as a chemical threat agent and a potential surrogate for nerve agents in the CounterACT program [26–29]. Table 1 summarizes the experimental design. The number of animals needed for each experiment (N) was calculated using the power analysis based on the magnitude of outcome parameters and published reports [15, 25, 30, 31]. For efficacy validation, diazepam was given by intramuscular (IM) injection under two different treatment regimen. The first is described as “early therapy” because diazepam was administered 10 min post-exposure to DFP. The second is described as “late therapy” because diazepam was administered at either 60 min or 120 min post-exposure to DFP. The late therapy time points were chosen because previous studies showed refractoriness to diazepam at these later post-exposure time points [15, 18–21, 24]. EEG seizure activity and behavioral seizure observations were recorded for 24 hours post-exposure DFP. Acute histological outcome was assessed at 72 h and chronic neurodegeneration was studied >3 months after exposure (data not shown).

We analyzed three primary outcome measures of treatment effectiveness: (i) anticonvulsant efficacy; (ii) neuroprotective efficacy; and (iii) prevention of neuroinflammation. The anticonvulsant efficacy of diazepam in terminating DFP-induced SE and seizure activity was assessed using four key parameters: (i) severity of behavioral seizures; (ii) frequency of electrographic spikes; (iii) cumulative duration of seizure activity; and (iv) latency to termination of seizure activity. EEG data was analyzed by Mini-analysis and Origin software. SE is considered terminated when the EEG returns to normal baseline or shows irregular spikes of <1 spike/s. Behavioral seizures are considered terminated when there was stage <2, normal behavior, or inactivity. The neuroprotective efficacy was assessed by histochemical staining and stereological analysis of brain sections using five specific markers [25]: (a) neuronal injury (FJB); (b) principal neuronal loss (neuronal nuclei, NeuN); (c) interneuron loss (parvalbumin, PV); and (d) astrocyte activation/injury (glial fibrillary acidic protein, GFAP); and microglia activation/injury (ionizing calcium binding adaptor

molecule-1, IBA1) in key brain regions including the amygdala, hippocampus, cortex, thalamus, and piriform cortex.

2.3. EEG electrode implantation

Rats were anesthetized with an intraperitoneal (IP) injection of a mixture of ketamine (100 mg/kg) and xylazine (10 mg/kg). Animals were fixed in the stereotaxic system. Stainless steel EEG recording electrodes (PlasticsOne, Roanoke, VA) were implanted on the surface of the brain over the right frontoparietal cortex and over the left cerebellum as a reference electrode. An intracranial depth electrode was placed into the right dentate gyrus as per the following coordinates with reference to the bregma using the Paxinos and Watson Rat Brain Atlas [32]: −4 mm anteroposterior, 2.3 mm mediolateral, and 3.4 mm dorsoventral. Rats were allowed to recover post-surgery for 1–2 weeks prior to experimentation.

2.4. DFP model of OP intoxication

DFP is a very similar structure to the nerve agents soman and sarin, hence it is widely accepted as a surrogate agent for nerve agents. DFP was purchased from Sigma-Aldrich (St. Louis, MO) and stored at 4°C. Dilutions were freshly prepared with ice-cold phosphate buffered saline prior to the study. We adapted a DFP protocol that was well established within the NIH CounterACT program [27–30]. Briefly, DFP is administered subcutaneously (3.2 mg/kg) in order to induce persistent seizures and SE in rats. There was a pretreatment with pyridostigmine bromide (0.026 mg/kg, IM) 30 min before DFP exposure. One minute following DFP exposure, rats were given 2-PAM (25 mg/kg, IM) and atropine methylnitrate (2 mg/kg, IP). This antidote regimen was given to increase the survival rates without affecting severity of seizures. This adapted regimen is consistent with protocols published by the U.S. Army Medical Research Institute of Chemical Defense [1,7,10].

2.5. Video-EEG and behavior recording

Behavior and EEG activity was monitored continuously for 24 h after DFP exposure to assess the progression of seizure activity and SE. A 1 h baseline EEG recording was conducted before each experiment by using a modern digital EEG system (Grass-Astromed, Warwick, RI). Rats were awake and freely moving in the cage fitted with swivels. DFP-induced EEG seizure activity was observed with the appearance of high amplitude (at least twice of the amplitude of the baseline wave) and repetitive discharges (>0.5 Hz). The severity of behavioral seizures were rated according to the Racine scale [33]: stage 0, normal behavioral activity; stage 1, chewing and facial twitches; stage 2, head nodding or shaking; stage 3, unilateral forelimb clonus without rearing, straub tail and extended body posture; stage 4, bilateral forelimb clonus plus rearing; and stage 5, wild jumping and tonic-clonic activity.

2.6. Diazepam treatment

The experimental design for drug administration and outcomes measurements are summarized in Fig. 1. Diazepam (DZ) was tested in a time-course design using 5 mg/kg (IM), which is considered the human equivalent dose for diazepam as an anticonvulsant for SE. In time-course study, rats were randomized into five groups (n = 8–14 per group):

control (no DFP), DFP, DFP+DZ (10 min), DFP+DZ (60 min), and DFP+DZ (120 min). The control group received a vehicle injection in a volume equal to DZ treated groups.

2.7. Perfusion and tissue processing

Rats were deeply anesthetized with ketamine (100 mg/kg)-xylazine (10 mg/kg) and were transcardially perfused with 0.9% saline followed by 4% paraformaldehyde solution in sodium phosphate buffer (PBS, pH 7.4). Following perfusion, the brain was carefully removed and post-fixed in 4% paraformaldehyde overnight at 4°C. Brain tissues were stored in PBS for 24 h. The brains were cryoprotected with 0.1 M phosphate buffer (pH 7.4) containing 20% sucrose for 72 h and rapidly frozen in isopentane pre-cooled to −70°C with dry ice. All brains were stored at −80°C before sectioning. Serial sections (30 μm) were cut coronally through the cerebrum containing the amygdala and the hippocampus, approximately from bregma −0.24 mm to −7.44 mm [32]. Every 20th section through the entire hippocampus was then selected from each rat in the group. Sections were taken at 600 μm intervals and processed for immunohistochemistry. Sections were stored in free-floating storage solution at −20°C before further processing. The sections of the first and second sets were mounted on microscope slides and stained with cresyl violet solution and Fluoro-jade B, respectively. The sections of the third, fourth, fifth and sixth sets were processed for NeuN, PV, GFAP and IBA1 immunoreactivity, respectively.

2.8. Fluoro-Jade B staining

The extent of acute neuronal damage after the DFP exposure was determined with FJB(+) staining as described previously [34, 35]. FJB is an anionic fluorescein derivative used for the histological labeling of the neurons that are undergoing degeneration or necrotic damage. Briefly, every 20th section of the rat brain was mounted on gelatin coated slides and air dried at room temperature overnight. The brain sections were serially hydrated with 100% ethanol, 70% ethanol and distilled water. Later the sections were processed in 0.06% potassium permanganate in distilled water for 10 min with slow shaking. Next, the sections were washed in distilled water and incubated in 0.004% FJB (Histo-Chem Inc., Jefferson, AR) in 0.1% acetic acid and distilled water for 30 min with slow shaking in the dark. Sections were then rinsed in distilled water and dried on a slide warmer at 55°C for 20 min in the dark. The brain sections were dehydrated in 50%, 70%, 90%, 100% ethanol serially, cleared in xylene and cover-slipped with DPX (Sigma). FJB-stained sections were stored in the dark to avoid the quenching of the fluorescence. The FJB(+) neurons in different regions of the hippocampus were counted via optical fractionator cell counting in the Visiopharm stereology system [36]. Evaluation of FJB (+) neurons in extra-hippocampal regions, including thalamus, hypothalamus, amygdala, piriform cortex, somatosensory cortex and entorhinal cortex was assessed by the neurodegeneration scoring method [37, 38]. Briefly, the tracings from the Nissl-stained sections were superimposed on the FJB-stained sections. The score system is as follows: 0 = no damage (0% of the neuronal population in FJB-stained); 1 = minimal damage (1–10%); 2 = mild damage (11–25%); 3 = moderate damage (26–45%); and 4 = severe damage (>45%). Qualitative assessment using this scale has been previously shown to produce results that are in agreement with quantitative assessments [39].

2.9. NeuN, PV, GFAP and IBA1 immunohistochemistry

Every 20th section through the entire rat hippocampus was selected for immunohistochemical analysis of neurodegeneration. Sections were taken at 600 μm intervals and processed for four cellular markers: (i) NeuN(+) expressing total principal cells [40–42]; (ii) PV(+) expressing inhibitory GABAergic interneurons [43,44]; (iii) GFAP(+) expressing astrocytes; and (iv) IBA1(+) expressing reactive microglia. This immunohistochemistry was performed using validated protocols as described previously [34, 36, 41–44]. Briefly, the sections were first processed for etching whereby the sections were rinsed in 0.1 M PBS solution and incubated with 20% methanol and 3% hydrogen peroxide for 30 min. The sections were then washed thrice with PBS. After inactivating the endogenous peroxidase activity with hydrogen peroxidase, they were washed in 0.1M PBS solution and treated with 10% normal horse or goat serum and 0.1% Triton X for 30 min to block non-specific binding of antibodies. Subsequently, sections were processed for specific immunoreactivity with the monoclonal mouse anti-NeuN antibodies (1:1000 in PBS, Millipore, Temecula, CA, USA), mouse anti-parvalbumin (1:2000 in PBS; Cat# P3088; Sigma-Aldrich, St. Louis, MO, USA) antibody solution, rabbit anti-GFAP antibodies (1:1000 in PBS; Cat# Z033429-2, Dako North America Inc., Carpinteria, CA, USA) and rabbit anti-IBA1 polyclonal antibodies (1:2000 in PBS; Wako Chemicals USA Inc, Richmond, VA, USA). The sections were incubated overnight in PBS containing the normal horse or goat serum, Triton X-100 and the specific NeuN, PV, GFAP and IBA1 antibodies at 4°C. Following, the sections were rinsed thrice in PBS, treated with the biotinylated anti-mouse or anti rabbit IgG secondary antibody solution (1:200, Vector) for 60 min and washed three times in PBS. Finally, the immunoreaction product was visualized according to the avidin-biotin complex (ABC) method [44] using the Vectastain elite ABC kit (Vector Lab, Burlingame, CA, USA) and peroxidase reaction was developed using 3', 3'-diaminobenzidine as a chromogen (Vector Lab, Burlingame, CA, USA) for 60 min, as per manufacturer's instructions. Following thorough washes in distilled water, all sections were mounted on gelatin-coated slides, air-dried, dehydrated in ethanol, cleared in xylene, and cover slipped (VWR, Radnor, PA, USA) with DPX (Sigma).

2.10. Neurostereology for quantification of surviving principal cells and interneurons

The total surviving NeuN(+) principal cells and PV(+) interneurons in the hippocampus subfields from various subgroups were quantified using a neurostereology protocol as described previously from our lab [36]. The dissector height is selected when 90% of cells in the field of the slice will be counted in the optical dissector cubic. The volume of any specific region of interest in rat can be found by utilizing the 10× objective lens in the Olympus BX53 microscope. To produce accurate volume estimation, at least 200 points were required to be counted in each region of interest. The absolute cell number counts and densities were calculated using the optical fractionator component in the Visiopharm stereology system [45–47].

2.11. Densitometric quantification of cellular inflammation

To determine the extent of reactive astrocytes and microglial proliferation after DFP exposure, area fraction analysis of GFAP(+) and IBA1(+) immunoreactive elements was

performed by using NIH Image J. One image for each slice (total 5) was taken in the same anatomic position in the closed location of each slice away from the bregma (e.g. bregma −3.00, −3.60, −4.20, −4.80, and −5.40 mm) for each subfield of the animal under 20× objective lens. Occasionally, images from 40× objective lens were used to verify the consistency of the results. For measurements of area fraction of sections, each image was converted to 16 bit grayscale and a threshold value was selected to keep all the GFAP/IBA1-immunopositive structures of soma and dendrites without any background noise [42]. The final image was carefully crosschecked with the original color-scale image by alternating the two images on the screen. The area occupied by the GFAP(+) or IBA1(+) expressing components in the gray image was then measured by selecting the Analyze Particles command in the ImageJ program using identical particle parameters. In this way, the area fraction of particle to total area checked was examined.

2.12. Statistical analysis

The statistical values are expressed as the mean ± S.E.M. Statistical comparisons of EEG spike counts, neuronal counts, densitometry data were performed with repeated-measures analysis of variance (ANOVA) followed by post hoc tests or with independent student's *t*-test, as appropriate. Behavioral seizure stage and incidence outcomes were compared with the nonparametric Kruskal-Wallis test followed by Mann-Whitney U test. In all statistical tests, the criterion for statistical significance was $p < 0.05$.

3. Results

3.1. Effect of early and late therapy with diazepam on DFP-induced seizures and SE

To investigate the time-dependent loss of DZ efficacy, we tested the drug with early (10 min) or late (60 or 120 min) therapy (Fig. 1). The progression of EEG seizure activity and behavioral seizures after DFP exposure are depicted in Fig. 2A. In the control group, epileptiform spikes began within 8 min after DFP exposure and progressed into rhythmic SE; generalized tonic-clonic behavioral seizure activity occurred in parallel with high amplitude continuous EEG discharges (Fig. 2A). The behavioral SE is described as intense unilateral or bilateral forelimb clonus, rearing, and falling (Fig. 2B). An expanded behavioral seizure activity rated by the Racine scale is shown in Fig. 2C. The electrographic and behavioral SE activity persisted for several hours after DFP exposure (Fig. 2BD). Diazepam was administered post-exposure at either 10 min, 60 min or 120 min. The overall survival rates for the treatment groups is listed in Table 1. DFP-induced mortality was prevented completely by early (10 min) administration of diazepam. The DZ-induced suppression of SE was time-dependent (Table 1). Diazepam treatment at 10 min post-DFP resulted in a rapid and effective termination of behavioral and electrographic SE (Fig. 2BCD). However, there was a seizure resurgence 2 h after early DZ treatment. When DZ was administered 60 min after DFP, seizures were reduced temporarily and then recurred with moderately intense SE (Fig. 2ABD). Diazepam treatment at 120 min post-DFP was not associated with significant termination of SE and seizure activity persisted for several hours (Fig. 2ABD).

3.2. Time-course of neuroprotective profile of diazepam treatment against DFP-induced NeuN(+) neurodegeneration

The protective effect of DZ was assessed 72 h post-exposure. To evaluate acute cell loss, we quantified the total surviving NeuN(+) principal cells in the hippocampus and other regions. Massive cell loss was noted in the principal cell layers of the hippocampus and dentate gyrus at 3 days after DFP exposure (Fig. 3A). The average absolute total cell count in a normal rat hippocampus including CA1, CA2, CA3 and DG subfields was 1,442,281 (Fig. 3B). The overall NeuN(+) neurodegeneration patterns in different regions of the hippocampus appeared symmetrical in both hemispheres, but variable within the different hippocampal subfields (Fig. 3A). The greatest damage was evident in the CA1, CA3, DG and DH subfields (Fig. 3A). Early administration of DZ conferred significant neuroprotection in the hippocampus (Fig. 3A). The stereological analysis of absolute total NueN(+) cells shows very minimal cell loss in rats treated with DZ 10 min post-exposure (Fig. 3BC). However, late therapy with DZ (either 60 min or 120 min) offered very limited neuroprotection in the hippocampus subfields as compared to DFP control group (Fig. 3BC). These results indicate that late therapy with diazepam provides very little protection against DFP-induced loss of principal cells in the brain.

3.3. Time-course of neuroprotective profile of diazepam against DFP-induced loss of PV(+) GABAergic interneurons

Inhibitory GABAergic PV(+) interneurons in the hippocampus are highly susceptible to OP intoxication. To examine whether DZ therapy was associated with protection of inhibitory interneurons, we performed immunohistological analysis of PV(+) interneurons in the hippocampal subfields. In all subgroups, PV(+) interneurons were present in the hilus and the granule cell layer of the dentate gyrus, and strata oriens, pyramidale and radiatum of the CA1, CA2 and CA3 subfields (Fig. 4A). The average total PV(+) cell number in the whole hippocampus was 53,362 (Fig. 4B). DFP caused a significant degeneration of PV(+) interneurons in all the hippocampal cell layers studied (Fig. 4B). The percentage analysis shows a relatively greater damage in the CA1, CA3, and DG layers (Fig. 4C). Diazepam treatment at 10 min post-exposure, but not at either 60 or 120 min post-exposure offered significant protection against the DFP-induced loss of interneurons in CA1, CA3, and DG subfields (Fig. 4BC). These results indicate that delayed/late therapy with DZ is associated with extensive degeneration of inhibitory interneurons in the hippocampus.

3.4. Time-course of protective effect of diazepam on DFP-induced FJB(+) acute neuronal damage in the hippocampus and amygdala

The FJB staining is a common histology technique used in evaluating the presence of acutely injured cells and neuronal degeneration in brain sections after brain injury models [35]. Rat brain sections isolated from the control group exhibited widespread FJB(+) fluorescence in the hippocampus and amygdala, indicating massive neuronal injury and degeneration of neurons (Fig. 5A). The total FJB(+) fluorescent (dying) neurons were counted by stereology technique (Fig. 5B). The change in the number of FJB(+) cells was expressed as percent protection after normalization of the values with the control group, as 100% injury (0% protection). FJB(+) cell numbers in rats treated with early therapy were

significantly lower compared to the control group (Fig. 5A). However, no significant differences in FJB(+) cells (Fig. 5B) and the degree of protection (Fig. 5C) were found between either late therapy group and DFP controls (Fig. 5A), indicating very little neuroprotection by DZ when administered in a delayed fashion.

3.5. Time-course of protective effect of diazepam on DFP-induced FJB(+) acute neuronal damage in the extra-hippocampal regions

We investigated the neurotoxic impact of DFP on neuronal degeneration in extra-hippocampal brain regions, including thalamus, hypothalamus, piriform cortex, somatosensory cortex and entorhinal cortex (Fig. 6A). To surpass the laborious stereology counts for numerous regions, we utilized a simple neuropathology-based scoring of neuronal damage in these regions. As shown in Fig. 7, extensive FJB(+) dying cells was evident in thalamus, piriform cortex, somatosensory cortex and entorhinal cortex. The hypothalamus had the lowest FJB(+) expressing cells compared to the other structures (Fig. 7). The extent of neurodegeneration was significantly lower in rats treated with DZ at 10 min post-exposure (Fig. 6B). However, there was no significant protection in rats that received DZ at 60 min or later post-exposure (Fig. 6B). These results suggest that early, but not late, therapy with DZ provides protection against DFP-induced acute neuronal injury and cell death in widespread regions in the brain.

3.6. Temporal profile of diazepam against DFP-induced GFAP(+) astrocytosis and neuroinflammation

The induction of a neuroinflammatory response is a common sequel after OP intoxication [62,63]. To determine the extent of DFP-induced reactive astrocytes that play key role in neuronal repair and inflammation, we examined astrocyte activation by GFAP(+) immunostaining of brain sections isolated at 3 days post-DFP exposure (Fig. 8A). The area fractionation values for GFAP-immunoreactive elements were calculated separately for each animal. In the hippocampus, reactive astrocytes were recognizable in all DFP-exposed groups, particularly in the CA1 and CA3 cell layer (Fig. 8A). Figure 8A shows the presence of enhanced reactive astrocytes, exhibited as swollen soma and shorter processes, in the hippocampus and amygdala regions after DFP exposure. Astrocytes clearly exhibited thicker and longer processes following DFP exposure, which upregulated the GFAP(+) expressing astrocytes within the CA1, CA3, DG subfields and amygdala (Fig. 8B). The GFAP(+) expression in the hippocampus and amygdala was significantly reduced in rats given early DZ, but no such protection was observed in rats treated in either late therapy scenario (60 or 120 min) (Fig. 8BC). These results suggest that delayed DZ administration provides very little protection against DFP-induced astrocytic activation and related inflammatory response.

3.7. Temporal profile of diazepam against DFP-induced IBA1(+) microgliosis and neuroinflammation

To determine the time-related protective effect of DZ on DFP-induced reactive microgliosis and inflammation, we performed IBA1(+) immunohistochemistry in the brain sections isolated from rats at 3 days after exposure. Our results revealed the presence of activated microglial cells in the hippocampal CA1, CA3 and DG subfields and amygdala after DFP

exposure (Fig. 9A). The activated microglial cells in the hippocampus exhibited swollen soma as well as shorter and stouter processes than normal microglial cells (Fig. 9A). Quantification of IBA1(+)-immunoreactive microglia revealed 140%–208% increase in brain regions, including amygdala and hippocampus subfields, following DFP exposure (Fig. 9C). The IBA1(+) microglial response was completely prevented in rats receiving early therapy, but not delayed (60 or 120 min) DZ administration (Fig. 9AB). These results indicate that delayed (60 min or later) administration of DZ provides limited or no protection against microglial proliferation and neuroinflammation after DFP exposure.

4. Discussion

The main finding of this study is that diazepam, when injected via the intramuscular route, can control DFP-induced SE and protect against neurodegeneration and inflammation when administered at an early (10 min) post-exposure time point. Diazepam was not effective when administered in a late therapy scenario, when administration occurred at either 60 min or 120 min post-exposure. The authors acknowledge published literature which confirms that the pharmacokinetics of diazepam is better controlled when administered intravenously, versus intramuscularly. However, current marketed therapies utilize an autoinjector, therefore the efficacy model utilized in this study is more relevant because the drug routes of administration are the same. Also significantly relevant to the study conclusion is the fact that the late therapy scenario is a realistic regimen to which new therapeutics should demonstrate efficacy because it reflects what is achievable in the field after a mass casualty OP exposure.

Here, we characterized the acute consequences of DFP-induced SE and investigated potential neuronal mechanisms that may underlie chronic morbidity in surviving animals. Our results confirm the diazepam refractoriness to DFP-induced SE and provide plausible mechanisms underlying such outcomes, including changes in inhibitory interneurons and inflammatory glial activation. These findings, while unsurprisingly similar to that observed in other animal models of SE [19,21–24], are notable because they suggest that drugs that terminate or protect against diazepam-refractory SE likely hold promise to treat nerve agent-induced SE.

Our findings are consistent with literature reports on the anticonvulsant efficacy of diazepam in pilocarpine model of SE [19–22]. However, there are several differences in experimental approach to diazepam testing. In our study, diazepam (5 mg/kg) was given intramuscularly 10 min, 60 min or 120 min after DFP and acute histology verified at 72 hours. Whereas in some studies [19], diazepam (10 mg/kg) was infused intravenously in pilocarpine model and neuropathology was assessed at 3 weeks. In other studies [21,22], a supra-therapeutic dose of diazepam (20 mg/kg) was given by IP injection in the pilocarpine model. Like the DFP-induced SE, pilocarpine produces persistent SE and neuropathology but the diazepam therapeutic outcomes are not comparable due to differences in the dose (5 mg/kg vs 20 mg/kg) and route of administration for delivering diazepam (IM injection vs IV infusion). Although diazepam exhibits erratic absorption and variable pharmacokinetics after IM injection compared to IV infusion, such therapy is clinically relevant and mimics the diazepam delivery from the IM autoinjectors. A better response was noted with delayed

administration of high-dose diazepam (20 mg/kg, ip) after pilocarpine-induced SE [20]. In addition, kainic acid–induced SE can be stopped by high-dose diazepam even when the drug is administered 3 hours after the onset of seizures [39]. Since the extent of neuronal damage increases with corresponding increase in the duration of SE, the utility of high doses of diazepam at delayed time points is uncertain. Moreover, such high doses could produce deep sedation, respiratory depression and adverse outcomes on survival. The refractoriness to benzodiazepines is a relative phenomenon [20, 24]. Consistent with such premise, diazepam temporarily reduced seizures but did not completely terminate them. Continuous seizure monitoring confirmed the seizure resurgence a few hours later in all diazepam-treated cohorts. Overall, these results confirm the reduced efficacy of benzodiazepines in terminating SE in animals and humans [16, 25, 49–52].

The mechanisms underlying the benzodiazepine refractoriness of SE remains unclear. Molecular and electrophysiological studies in animal models of SE indicate that such phenomenon may involve internalization and downregulation of synaptic GABA-A receptors (primary targets of benzodiazepines) from neuronal membrane sites, or other dysfunctions in GABAergic synaptic transmission that manifest as the seizures progress [17, 52–57]. It is known that postsynaptic inhibition displays a high degree of plasticity in the hippocampus in that during prolonged epileptiform bursting, the rate of synaptic GABA-A receptor internalization increases rapidly, the subunit composition of these receptors swiftly changes (downregulation of benzodiazepine-sensitive γ2-subunits), and benzodiazepines ultimately lose efficacy due to limited network inhibition to shunt excessive seizure discharges [55]. A significant decrease in the surface expression of γ2-containing synaptic GABA-A receptors (targets for benzodiazepines) is observed during persistent SE, whereas no such change is evident in δ-containing extrasynaptic GABA-A receptors (targets for neurosteroids) [58–61].

Neuropathology data reported in the literature suggests that extensive loss of principal neurons and interneurons are hallmark features of OP intoxication [37,48]. In this study, delayed diazepam therapy was associated with very limited protection against DFP-induced neuronal injury and loss of NeuN(+) principal cells and PV(+) interneurons. The functional correlation of loss of interneurons has not been studied in detail in OP intoxication. PV(+) interneurons constitute about 40% of total GABAergic interneurons and play a critical role in regulating the inhibitory strength of neuronal circuits. These interneurons are present in the brain structures that are critical for excitability and seizure susceptibility such as: hippocampus, amygdala and other limbic regions. Our results show that DFP-induced SE results in a substantial loss of PV(+) interneurons in all regions of the hippocampus in the control group and in late therapy diazepam treated groups. Therefore, when diazepam is administered at delayed time points (>60 min), it may be ineffective due to SE-induced loss of inhibitory interneurons and reduction in drug target receptors [52, 55, 56].

Persistent activation of inflammatory responses is another hallmark feature of OP intoxication [48, 62,63]. Early administration of diazepam is required to diminish brain inflammatory responses. Immunostaining with GFAP or IBA1 revealed significant proliferation and morphological changes in reactive astrocytes and activated microglia in many brain regions. Activated glial cells increase the levels of inflammatory cytokines, such

as interleukin-6 and tumor necrosis factor. Our results show that there were differences in microglial and astrocytic reactivity in different brain regions (Fig. 8 and Fig. 9). The roles of astrocytosis and microgliosis in brain damage are complex and temporally dynamic including both beneficial and detrimental effects depending on which cytokine(s) are released. In addition, the upregulation of astrocytic and microglial markers is strongly correlated with functional and behavioral deficits [64]. The hypertrophic deformation of microglia and astrocytes create an ectopic glial scaffold that promotes the aberrant growth of basal dendrites into the hilus, which could create a recurrent excitatory circuit to facilitate seizures. However, the actual impact of microglia on chronic neuronal damage, as well as their influence on the reparative or injury-healing actions following OP intoxication is not yet fully understood [65–70].

Benzodiazepines are safe treatment options for acute seizure and SE, which is a medical emergency associated with significant neurological morbidity and mortality [16, 50, 71–72]. Early treatment has significant protective action including better survival rate and faster SE termination. However, a short window of opportunity exists when SE is effectively controlled by benzodiazepine therapy. After that, multiple pathological mechanisms quickly trigger to create benzodiazepine-refractory state that make seizures increasingly more difficult to control with high risk for long-term damage [71, 72]. Therefore, diazepam is less optimal for the treatment of nerve agent-induced seizures considering the therapeutic window of a delayed post-exposure scenario. Repeated dosing or high doses of benzodiazepines may offer little benefit from the potential risks including developing epilepsy and cognitive dysfunction [73,74]. Therefore, novel anticonvulsants or combination regimen that target extrasynaptic GABA-A receptors may be more effective approach to controlling nerve agent-induced SE and brain damage [75–78].

In conclusion, these results demonstrate that the DFP model of OP exposure in rats replicates many features of nerve agent exposure, including benzodiazepine-resistant seizures, SE and neuronal damage. The DFP-induced SE, neurodegeneration, and neuroinflammation become progressively resistant to treatment with diazepam, confirming the benzodiazepine-refractory SE and neuropathology. The outcomes of prolonged DFP-induced SE are similar to those of other models of SE including rapid development of diazepam refractoriness, potential interneuron dysfunction and glia-mediated inflammatory response. These observations support the possibility that nerve agent-induced seizures may respond to novel anticonvulsants effective in other models, such as neurosteroids [76,77].

Supplementary Material

Refer to Web version on PubMed Central for supplementary material.

Acknowledgments

This work was supported by the CounterACT Program, U.S. National Institutes of Health, Office of the Director and the National Institute of Neurologic Disorders and Stroke [Grants U01 NS083460 & R21 NS099009]. We thank Victoria Golub, Jenessa Short, and Ryan Cieker for excellent help with neurostereology.

Abbreviations

CNS	central nervous system
SE	status epilepticus
EEG	Electroencephalogram
DFP	diisopropylfluorophosphate
FJB	fluoro-jade B
NeuN	neuronal nuclei
GFAP	glial fibrillary acidic protein
PV	parvalbumin
IBA1	ionized calcium binding adaptor molecule-1

References

1. McDonough JH Jr, Shih TM. Neuropharmacological mechanisms of nerve agent-induced seizure and neuropathology. Neuroscience and biobehavioral reviews. 1997; 21:559–579. [PubMed: 9353792]
2. Shih TM, Duniho SM, McDonough JH. Control of nerve agent-induced seizures is critical for neuroprotection and survival. Toxicology and applied pharmacology. 2003; 188:69–80. [PubMed: 12691725]
3. Dolgin E. Syrian gas attack reinforces need for better anti-sarin drugs. Nature medicine. 2013; 19:1194–1195.
4. Abou-Donia MB, Siracuse B, Gupta N, Sobel Sokol A. Sarin (GB, O-isopropyl methylphosphonofluoridate) neurotoxicity: critical review. Critical reviews in toxicology. 2016; 46:845–875. [PubMed: 27705071]
5. Bajgar J, Fusek J, Kassa J, Jun D, Kuca K, Hajek P. An attempt to assess functionally minimal acetylcholinesterase activity necessary for survival of rats intoxicated with nerve agents. Chemicobiological interactions. 2008; 175:281–285.
6. Nozaki H, Hori S, Shinozawa Y, Fujishima S, Takuma K, Sagoh M, Kimura H, Ohki T, Suzuki M, Aikawa N. Secondary exposure of medical staff to sarin vapor in the emergency room. Intensive care medicine. 1995; 21:1032–1035. [PubMed: 8750130]
7. Shih TM, McDonough JH Jr. Neurochemical mechanisms in soman-induced seizures. Journal of applied toxicology. 1997; 17:255–264. [PubMed: 9285539]
8. Reddy DS, Colman E. A Comparative Toxidrome Analysis of Human Organophosphate and Nerve Agent Poisonings Using Social Media. Clinical and translational science. 2017; 10:225–230. [PubMed: 28238224]
9. Chen JW, Wasterlain CG. Status epilepticus: pathophysiology and management in adults. The Lancet. Neurology. 2006; 5:246–256. [PubMed: 16488380]
10. Shih T, McDonough JH Jr, Koplovitz I. Anticonvulsants for soman-induced seizure activity. Journal of biomedical science. 1999; 6:86–96. [PubMed: 10087439]
11. Skovira JW, McDonough JH, Shih TM. Protection against sarin-induced seizures in rats by direct brain microinjection of scopolamine, midazolam or MK-801. Journal of molecular neuroscience. 2010; 40:56–62. [PubMed: 19690985]
12. Hayward IJ, Wall HG, Jaax NK, Wade JV, Marlow DD, Nold JB. Decreased brain pathology in organophosphate-exposed rhesus monkeys following benzodiazepine therapy. Journal of the neurological sciences. 1990; 98:99–106. [PubMed: 2230834]

13. Capacio BR, Whalley CE, Byers CE, McDonough JH. Intramuscular diazepam pharmacokinetics in soman-exposed guinea pigs. Journal of applied toxicology. 2001; 21(Suppl 1):S67–74. [PubMed: 11920923]
14. McDonough JH, McMonagle JD, Shih TM. Time-dependent reduction in the anticonvulsant effectiveness of diazepam against soman-induced seizures in guinea pigs. Drug and chemical toxicology. 2010; 33:279–283. [PubMed: 20429808]
15. Apland JP, Aroniadou-Anderjaska V, Figueiredo TH, Rossetti F, Miller SL, Braga MF. The limitations of diazepam as a treatment for nerve agent-induced seizures and neuropathology in rats: comparison with UBP302. The Journal of pharmacology and experimental therapeutics. 2014; 351:359–372. [PubMed: 25157087]
16. Reddy SD, Reddy DS. Midazolam as an anticonvulsant antidote for organophosphate intoxication--A pharmacotherapeutic appraisal. Epilepsia. 2015; 56:813–821. [PubMed: 26032507]
17. Wasterlain CG, Chen JW. Mechanistic and pharmacologic aspects of status epilepticus and its treatment with new antiepileptic drugs. Epilepsia. 2008; 49(Suppl 9):63–73. [PubMed: 19087119]
18. Goodkin HP, Liu X, Holmes GL. Diazepam terminates brief but not prolonged seizures in young, naive rats. Epilepsia. 2003; 44:1109–1112. [PubMed: 12887445]
19. Klitgaard H, Matagne A, Vanneste-Goemaere J, Margineanu DG. Pilocarpine-induced epileptogenesis in the rat: impact of initial duration of status epilepticus on electrophysiological and neuropathological alterations. Epilepsy research. 2002; 51:93–107. [PubMed: 12350385]
20. Gao X-G, Liu Y, Liu X-Z. Treatment of late lithium-pilocarpine-induced status epilepticus with diazepam. Epilepsy research. 2007; 74:126–130. [PubMed: 17398071]
21. Biagini G, Baldelli E, Longo D, Contri MB, Guerrini U, Sironi L, Gelosa P, Zini I, Ragsdale DS, Avoli M. Proepileptic influence of a focal vascular lesion affecting entorhinal cortex-CA3 connections after status epilepticus. Journal of neuropathology and experimental neurology. 2008; 67:687–701. [PubMed: 18596544]
22. Gualtieri F, Curia G, Marinelli C, Biagini G. Increased perivascular laminin predicts damage to astrocytes in CA3 and piriform cortex following chemoconvulsive treatments. Neuroscience. 2012; 218:278–294. [PubMed: 22609936]
23. Lucchi C, Curia G, Vinet J, Gualtieri F, Bresciani E, Locatelli V, Torsello A, Biagini G. Protective but not anticonvulsant effects of ghrelin and JMV-1843 in the pilocarpine model of Status epilepticus. PLoS One. 2013; 8:e72716. [PubMed: 24015271]
24. Todorovic MS, Cowan ML, Balint CA, Sun C, Kapur J. Characterization of status epilepticus induced by two organophosphates in rats. Epilepsy research. 2012; 101:268–276. [PubMed: 22578704]
25. Wu X, Kuruba R, Reddy DS. Midazolam-resistant seizures and brain injury following acute intoxication of diisopropylfluorophosphate, an organophosphate pesticide and surrogate for nerve agents. Journal of pharmacology and experimental therapeutis. 2018; 365:000–000.
26. Jett DA, Yeung DT. The CounterACT Research Network: basic mechanisms and practical applications. Proceeding of American Thoracic Society. 2010; 7:254–256.
27. Deshpande LS, Carter DS, Blair RE, DeLorenzo RJ. Development of a prolonged calcium plateau in hippocampal neurons in rats surviving status epilepticus induced by the organophosphate diisopropylfluorophosphate. Toxicological sciences. 2010; 116:623–631. [PubMed: 20498005]
28. Pouliot W, Bealer SL, Roach B, Dudek FE. A rodent model of human organophosphate exposure producing status epilepticus and neuropathology. Neurotoxicology. 2016; 56:196–203. [PubMed: 27527991]
29. Siso S, Hobson BA, Harvey DJ, Bruun DA, Rowland DJ, Garbow JR, Lein PJ. Spatiotemporal Progression and Remission of Lesions in the Rat Brain Following Acute Intoxication With Diisopropylfluorophosphate. Toxicological sciences. 2017; 157:330–341. [PubMed: 28329845]
30. Kim YB, Hur GH, Shin S, Sok DE, Kang JK, Lee YS. Organophosphate-induced brain injuries: delayed apoptosis mediated by nitric oxide. Environmental toxicology and pharmacology. 1999; 7:147–152. [PubMed: 21781920]
31. Shih TM, Koviak TA, Capacio BR. Anticonvulsants for poisoning by the organophosphorus compound soman: pharmacological mechanisms. Neuroscience and biobehavioral reviews. 1991; 15:349–362. [PubMed: 1683477]

32. PaxinosG, , WatsonC. The rat brain in stereotaxic coordinates6. Academic Press; New York: 2007
33. Racine RJ. Modification of seizure activity by electrical stimulation. II. Motor seizure. Electroencephalography and clinical neurophysiology. 1972; 32:281–294. [PubMed: 4110397]
34. Rao MS, Hattiangady B, Reddy DS, Shetty AK. Hippocampal neurodegeneration, spontaneous seizures, and mossy fiber sprouting in the F344 rat model of temporal lobe epilepsy. Journal of Neuroscience Research. 2006; 83:1088–1105. [PubMed: 16493685]
35. Schmued LC, Albertson C, Slikker W Jr. Fluoro-Jade: a novel fluorochrome for the sensitive and reliable histochemical localization of neuronal degeneration. Brain research. 1997; 751:37–46. [PubMed: 9098566]
36. Golub VM, Brewer J, Wu X, Kuruba R, Short J, Manchi M, Swonke M, Younus I, Reddy DS. Neurostereology protocol for unbiased quantification of neuronal injury and neurodegeneration. Frontiers in Aging Neuroscience. 2015; 7:196. [PubMed: 26582988]
37. Apland JP, Figueiredo TH, Qashu F, Aroniadou-Anderjaska V, Souza AP, Braga MF. Higher susceptibility of the ventral versus the dorsal hippocampus and the posteroventral versus anterodorsal amygdala to soman-induced neuropathology. Neurotoxicology. 2010; 31:485–492. [PubMed: 20570628]
38. Myhrer T, Andersen JM, Nguyen NH, Aas P. Soman-induced convulsions in rats terminated with pharmacological agents after 45 min: neuropathology and cognitive performance. Neurotoxicology. 2005; 26:39–48. [PubMed: 15527872]
39. Qashu F, Figueiredo TH, Aroniadou-Anderjaska V, Apland JP, Braga MF. Diazepam administration after prolonged status epilepticus reduces neurodegeneration in the amygdala but not in the hippocampus during epileptogenesis. Amino Acids. 2010; 38:189–197. [PubMed: 19127342]
40. Mullen RJ, Buck CR, Smith AM. NeuN, a neuronal specific nuclear protein in vertebrates. Development. 1992; 116:201–211. [PubMed: 1483388]
41. Hattiangady B, Kuruba R, Shetty AK. Acute seizures in old age leads to a greater loss of CA1 pyramidal neurons, an increased propensity for developing chronic TLE and a severe cognitive dysfunction. Aging and disease. 2011; 2:1–17. [PubMed: 21339903]
42. Shetty AK, Rao MS, Hattiangady B, Zaman V, Shetty GA. Hippocampal neurotrophin levels after injury: Relationship to the age of the hippocampus at the time of injury. Journal of Neuroscience Research. 2004; 78:520–532. [PubMed: 15468179]
43. Megahed T, Hattiangady B, Shuai B, Shetty AK. Parvalbumin and neuropeptide Y expressing hippocampal GABA-ergic inhibitory interneuron numbers decline in a model of Gulf War illness. Frontiers in cellular neuroscience 8. 2005; 8:447.
44. Kuruba R, Hattiangady B, Parihar VK, Shuai B, Shetty AK. Differential susceptibility of interneurons expressing neuropeptide Y or parvalbumin in the aged hippocampus to acute seizure activity. PloS one. 2011; 6:e24493. [PubMed: 21915341]
45. West MJ. Introduction to stereology. Cold Spring Harbor protocols. 2012; 2012
46. West MJ. Getting started in stereology. Cold Spring Harbor protocols. 2013; 2013:287–297. [PubMed: 23547151]
47. Boyce RW, Dorph-Petersen KA, Lyck L, Gundersen HJ. Design-based stereology: introduction to basic concepts and practical approaches for estimation of cell number. Toxicologic pathology. 2010; 38:1011–1025. [PubMed: 21030683]
48. Li Y, Lein PJ, Liu C, Bruun DA, Tewolde T, Ford G, Ford BD. Spatiotemporal pattern of neuronal injury induced by DFP in rats: a model for delayed neuronal cell death following acute OP intoxication. Toxicology and applied pharmacology. 2011; 253:261–269. [PubMed: 21513723]
49. Walton NY, Treiman DM. Response of status epilepticus induced by lithium and pilocarpine to treatment with diazepam. Experimental neurology. 1988; 101:267–275. [PubMed: 3396644]
50. Shorvon S. The management of status epilepticus. Journal of neurology, neurosurgery, and psychiatry. 2001; 70(Suppl 2):II22–27.
51. Goodkin HP, Kapur J. The impact of diazepam's discovery on the treatment and understanding of status epilepticus. Epilepsia. 2009; 50:2011–2018. [PubMed: 19674049]
52. Deeb TZ, Maguire J, Moss SJ. Possible alterations in GABA-A receptor signaling that underlie benzodiazepine-resistant seizures. Epilepsia. 2012; 53(Suppl 9):79–88.

53. Goodkin HP, Joshi S, Mtchedlishvili Z, Brar J, Kapur J. Subunit-specific trafficking of GABA(A) receptors during status epilepticus. The Journal of Neuroscience. 2008; 28:2527–2538. [PubMed: 18322097]
54. Goodkin HP, Sun C, Yeh JL, Mangan PS, Kapur J. GABA-A receptor internalization during seizures. Epilepsia. 2007; 48(Suppl 5):109–113. [PubMed: 17910589]
55. Goodkin HP, Yeh JL, Kapur J. Status epilepticus increases the intracellular accumulation of GABAA receptors. The Journal of neuroscience. 2005; 25:5511–5520. [PubMed: 15944379]
56. Naylor DE, Liu H, Wasterlain CG. Trafficking of GABA-A receptors, loss of inhibition, and a mechanism for pharmacoresistance in status epilepticus. The Journal of neuroscience. 2005; 25:7724–7733. [PubMed: 16120773]
57. Vinkers CH, Olivier B. Mechanisms underlying tolerance after long-term benzodiazepine use: A future for subtype-selective GABA-A receptor modulators? Advances in pharmacological sciences. 2012; 2012:416864. [PubMed: 22536226]
58. Carver CM, Reddy DS. Neurosteroid structure-activity relationships for functional activation of extrasynaptic δGABA-A receptors. The Journal of pharmacology and experimental therapeutics. 2016; 357:188–204. [PubMed: 26857959]
59. Chuang SH, Reddy DS. Genetic and molecular regulation of extrasynaptic GABA-A receptors in the brain: Therapeutic insights for epilepsy. Journal of pharmacology and experimental therapeutics. 2018; 364:180–197. [PubMed: 29142081]
60. Reddy DS. GABA-A receptors mediate tonic inhibition and neurosteroid sensitivity in the brain. Vitamins and hormones. 2018; 107:177–191. [PubMed: 29544630]
61. Reddy SD, Younus I, Clossen BL, Reddy DS. Antiseizure activity of midazolam in mice lacking delta-subunit extrasynaptic GABA-A receptors. The Journal of pharmacology and experimental therapeutics. 2015; 353:517–528. [PubMed: 25784648]
62. de Araujo Furtado M, Rossetti F, Chanda S, Yourick D. Exposure to nerve agents: from status epilepticus to neuroinflammation, brain damage, neurogenesis and epilepsy. Neurotoxicology. 2012; 33:1476–1490. [PubMed: 23000013]
63. Banks CN, Lein PJ. A review of experimental evidence linking neurotoxic organophosphorus compounds and inflammation. Neurotoxicology. 2012; 33:575–584. [PubMed: 22342984]
64. Loane DJ, Byrnes KR. Role of microglia in neurotrauma. Neurotherapeutics. 2010; 7:366–377. [PubMed: 20880501]
65. Ribak CE, Tran PH, Spigelman I, Okazaki MM, Nadler JV. Status epilepticus-induced hilar basal dendrites on rodent granule cells contribute to recurrent excitatory circuitry. The Journal of comparative neurology. 2000; 428:240–253. [PubMed: 11064364]
66. De Simoni MG, Perego C, Ravizza T, Moneta D, Conti M, Marchesi F, De Luigi A, Garattini S, Vezzani A. Inflammatory cytokines and related genes are induced in the rat hippocampus by limbic status epilepticus. The European journal of neuroscience. 2000; 12:2623–2633. [PubMed: 10947836]
67. Heida JG, Pittman QJ. Causal links between brain cytokines and experimental febrile convulsions in the rat. Epilepsia. 2005; 46:1906–1913. [PubMed: 16393156]
68. Dube C, Vezzani A, Behrens M, Bartfai T, Baram TZ. Interleukin-1beta contributes to the generation of experimental febrile seizures. Annals of neurology. 2005; 57:152–155. [PubMed: 15622539]
69. Bartfai T, Sanchez-Alavez M, Andell-Jonsson S, Schultzberg M, Vezzani A, Danielsson E, Conti B. Interleukin-1 system in CNS stress: seizures, fever, and neurotrauma. Annals of the New York Academy of Sciences. 2007; 1113:173–177. [PubMed: 17656565]
70. Vezzani A. Epilepsy and inflammation in the brain: overview and pathophysiology. Epilepsy currents. 2014; 14:3–7. [PubMed: 24955068]
71. Naylor D. Treating acute seizures with benzodiazepines: does seizure duration matter? Epileptic disorders. 2014; 16:S69–S83. [PubMed: 25323468]
72. Niquet J, Baldwin R, Suchomelova L, Lumley L, Naylor D, Eavey R, Wasterlain CG. Benzodiazepine-refractory status epilepticus: pathophysiology and principles of treatment. Annals of the New York academy of sciences. 2016; 1378:166–173. [PubMed: 27392038]

73. Lhatoo SD, Johnson AL, Goodridge DM, MacDonald BK, Sander JW, Shorvon SD. Mortality in epilepsy in the first 11 to 14 years after diagnosis: multivariate analysis of a long-term, prospective, population-based cohort. Annals of neurology. 2001; 49:336–344. [PubMed: 11261508]

74. Shrot S, Ramaty E, Biala Y, Bar-Klein G, Daninos M, Kamintsky L, Makarovsky I, Statlender L, Rosman Y, Krivoy A, Lavon O, Kassirer M, Friedman A, Yaari Y. Prevention of organophosphate-induced chronic epilepsy by early benzodiazepine treatment. Toxicology. 2014; 323:19–25. [PubMed: 24881594]

75. Reddy DS. Clinical pharmacology of current antiepileptic drugs. International Journal of Pharmaceutical Sciences and Nanotechnology. 2014; 7:2305–2319.

76. Reddy DS. Neurosteroids for the potential protection of humans against organophosphate toxicity. Annals of the New York Academy of Sciences. 2016; 1378:25–32. [PubMed: 27450921]

77. Reddy DS, Estes WA. Clinical potential of neurosteroids for CNS disorders. Trends in pharmacological sciences. 2016; 37:543–561. [PubMed: 27156439]

78. Younus I, Reddy DS. A resurging boom in new drugs for epilepsy and brain disorders. Expert review of clinical pharmacology. 2018; 11:27–45. [PubMed: 28956955]

HIGHLIGHTS

- Nerve agents produce lethal seizures and status epilepticus (SE).
- Evidence suggests progressive loss of efficacy of benzodiazepines as anticonvulsants.
- Here, we confirm diazepam-resistant SE and brain injury after OP intoxication.
- Neurodegeneration of interneurons and inflammatory glial response plays a key role in benzodiazepines refractoriness of SE.

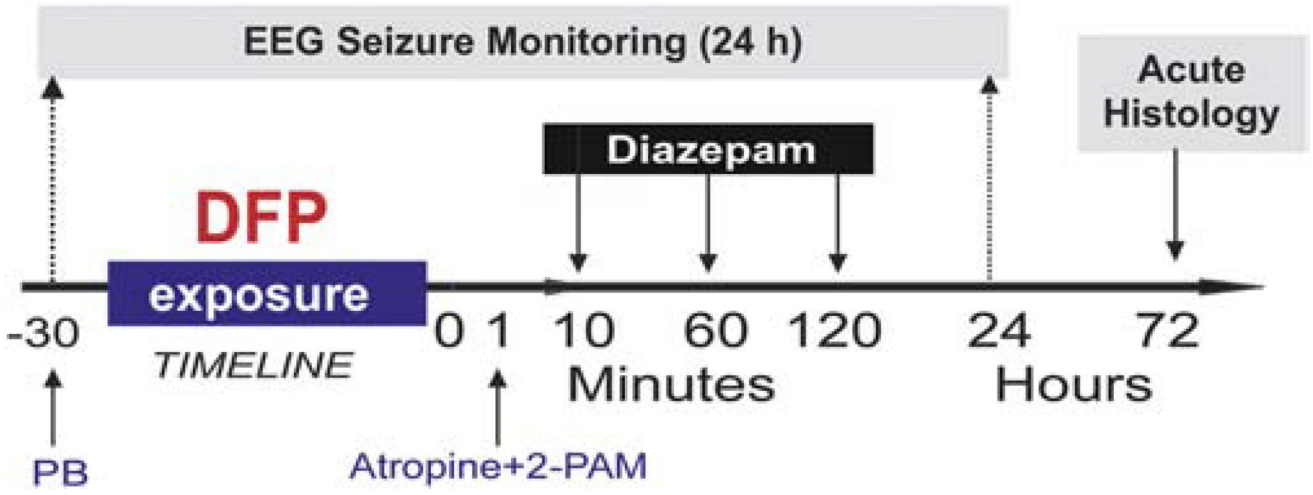

Fig. 1. Overall experimental protocol of the diisopropylfluorophosphate (DFP) model in rats

Timeline 0 refers to DFP exposure. Pyridostigmine bromide (PB) was given 30 min prior to DFP exposure. Atropine and 2-PAM (pralidoxime) were given within 1 min after DFP. Rats were monitored continuously for 24 h by video-EEG recording. Animals were performed 72 hours after DFP for histology. Diazepam (5 mg/kg, IM) was given at 10, 60 or 120 min after DFP exposure.

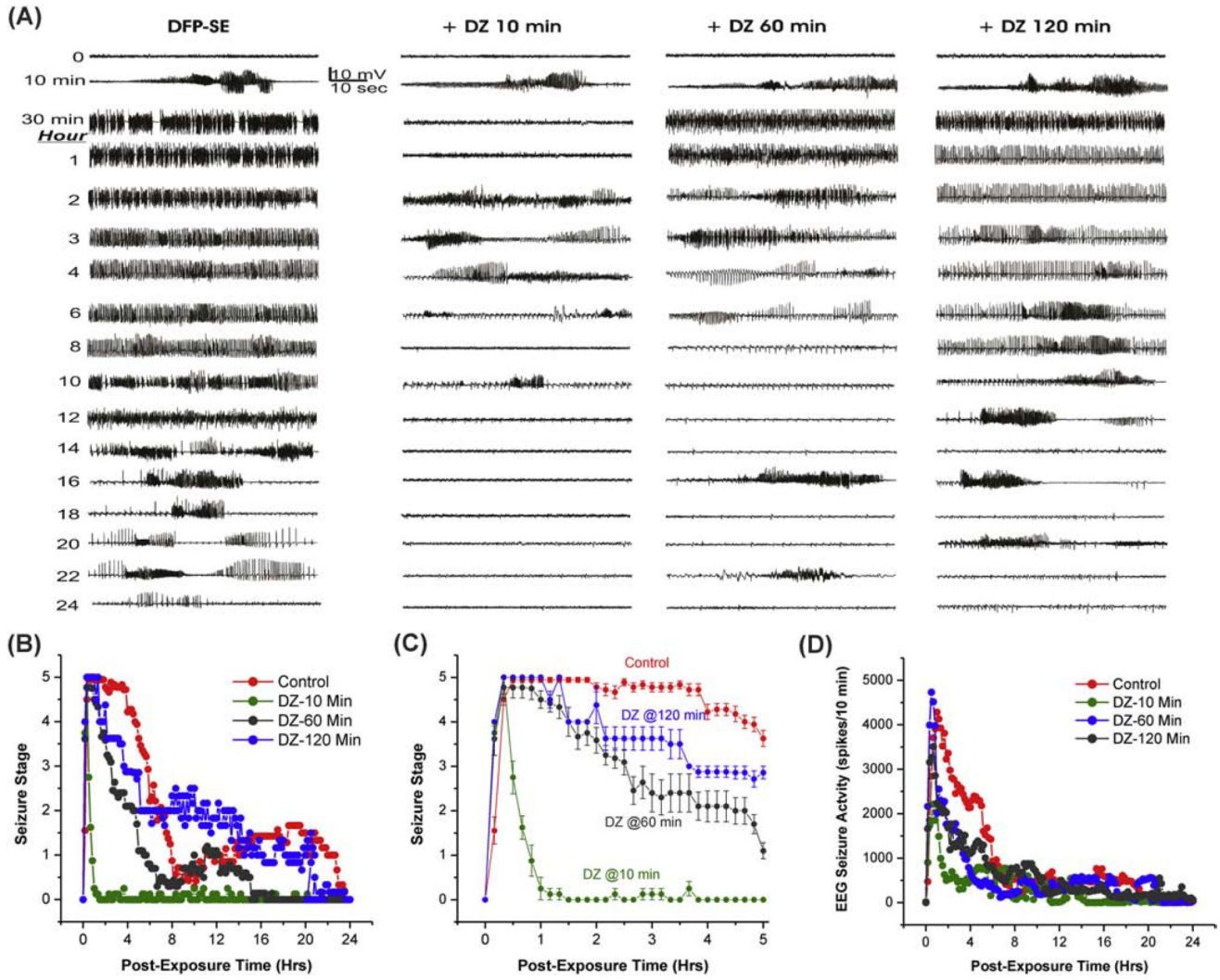

Fig. 2. Time-course of diazepam (5 mg/kg, IM) effect against DFP-induced SE in rats

(***A***) Time-course of EEG seizure activity. Traces represent 1-min epochs from a depth electrode in the hippocampus in rats. (B) Time-course of behavioral seizure suppression by treatment (10, 60 & 120-min after DFP) for 24 h. (C) Expanded version of behavioral seizure suppression during 5-h period. (D) Time-course of EEG seizure suppression by diazepam therapy. Rats were monitored for 24 h after DFP exposure. Each point represent mean response at 10-min intervals (n=5 to 11 rats per group).

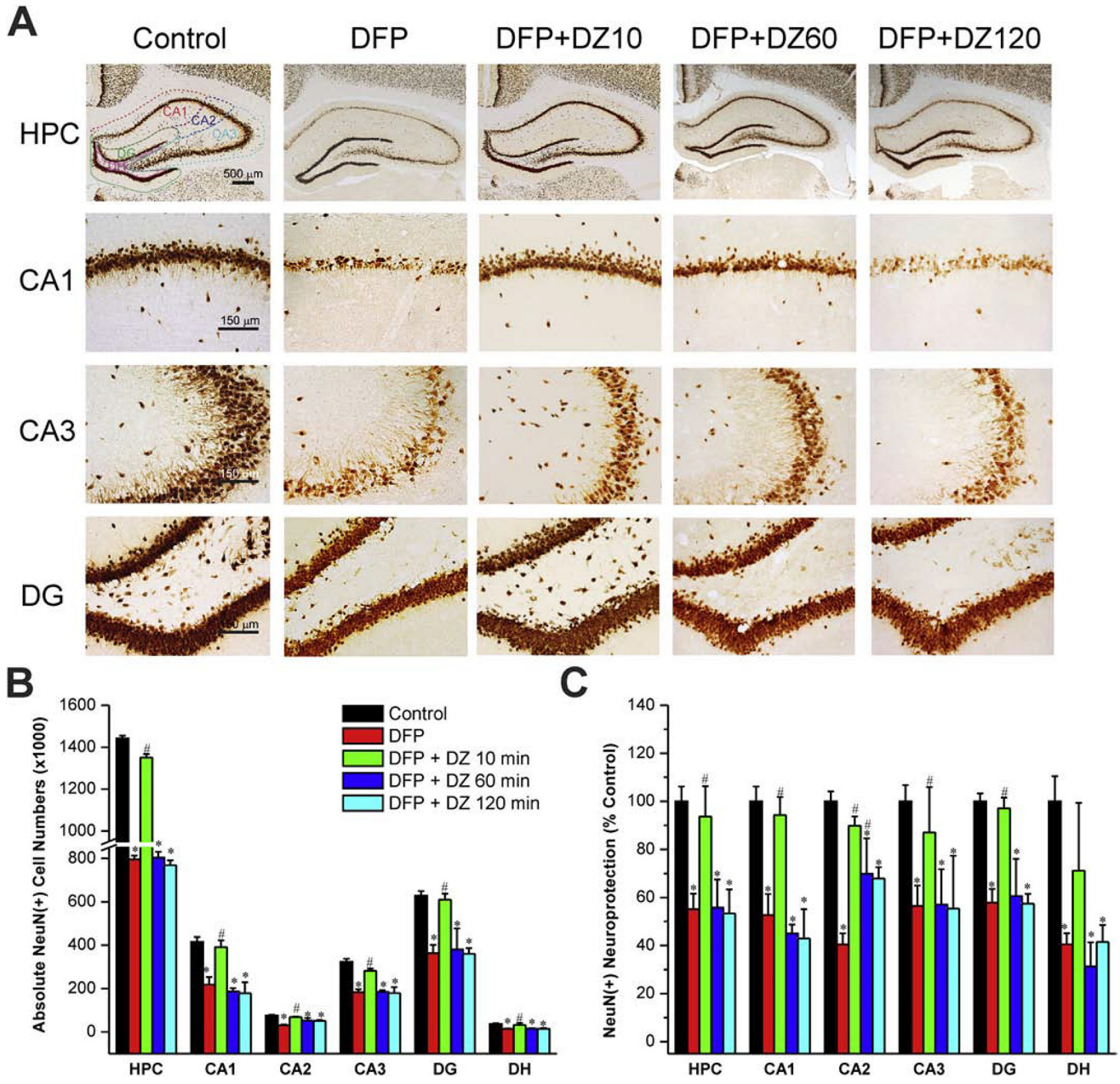

Fig. 3. Time-course profile of diazepam (5 mg/kg, IM) on DFP-induced loss of NeuN(+) principle neurons in the hippocampus (HPC)

(A) Representative sections of NeuN(+) immunostaining in animals with or without diazepam at 10, 60 or 120 min post-DFP in the hippocampus subfields. (N) The bar graph depict stereological quantification of absolute NeuN(+) cell numbers in the hippocampus subfields. (C) Percent protection of NeuN(+) cells in various subgroups in the hippocampus subfields. Values represent the mean ± SEM (n=5–8 rats per group). *p<0.05 vs control (no DFP); #p<0.05 vs DFP group (ANOVA and post hoc unpaired student *t*-test).

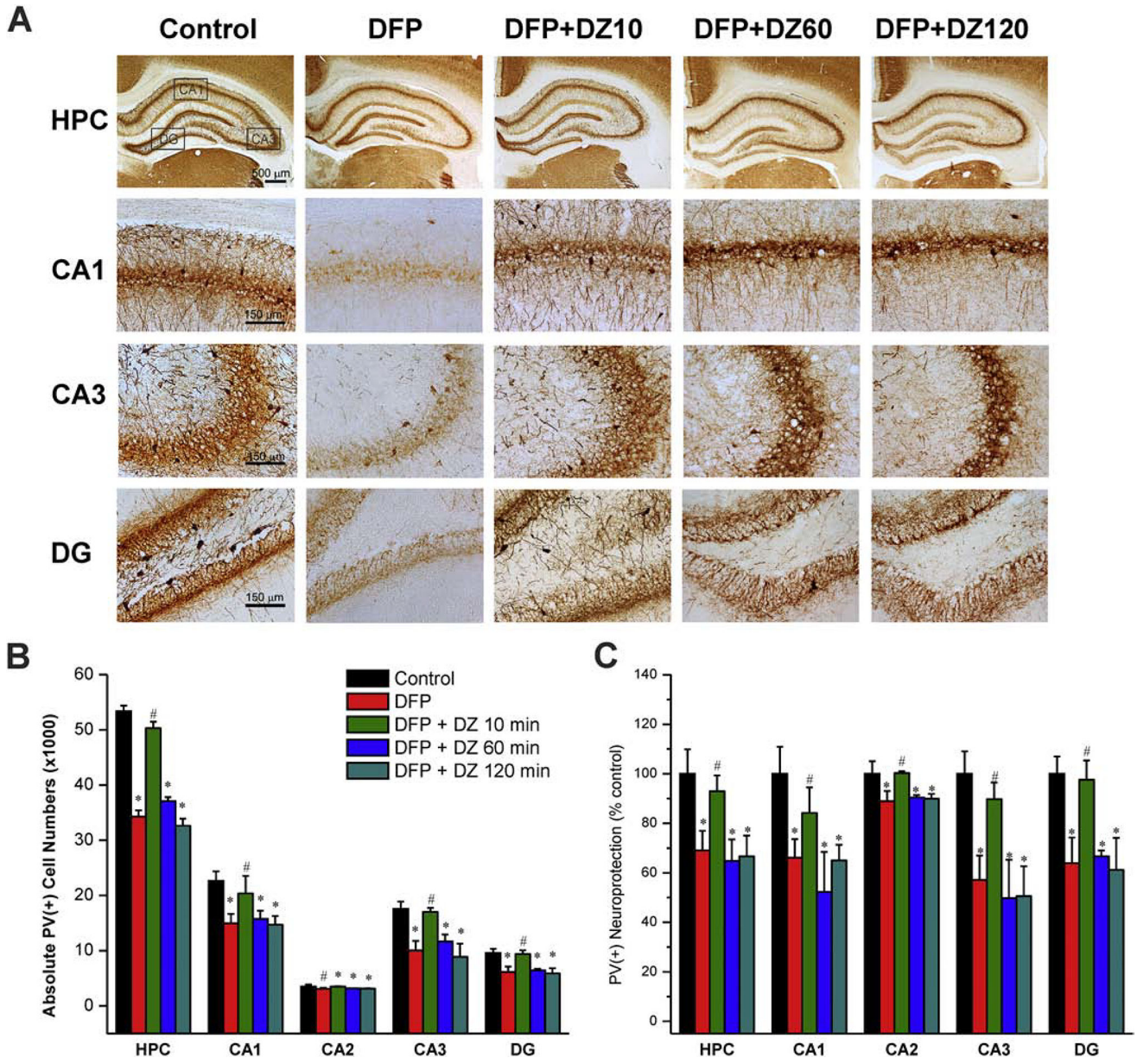

Fig. 4. Effect of diazepam (5 mg/kg, IM) on DFP-induced loss of PV(+) GABAergic interneurons in the hippocampus (HPC)

(A) Representative sections of PV(+) immunostaining in animals with or without diazepam at 10, 60 or 120 min post-DFP in the hippocampus subfields. (B) The bar graph depict stereological quantification of absolute PV(+) cell numbers in the hippocampus subfields. (C) Percent protection of PV(+) cells in various subgroups in the hippocampus subfields. Values represent the mean ± SEM (n=5–8 rats). *p<0.05 vs control (no DFP); #p<0.05 vs DFP group (ANOVA and post hoc unpaired student *t*-test).

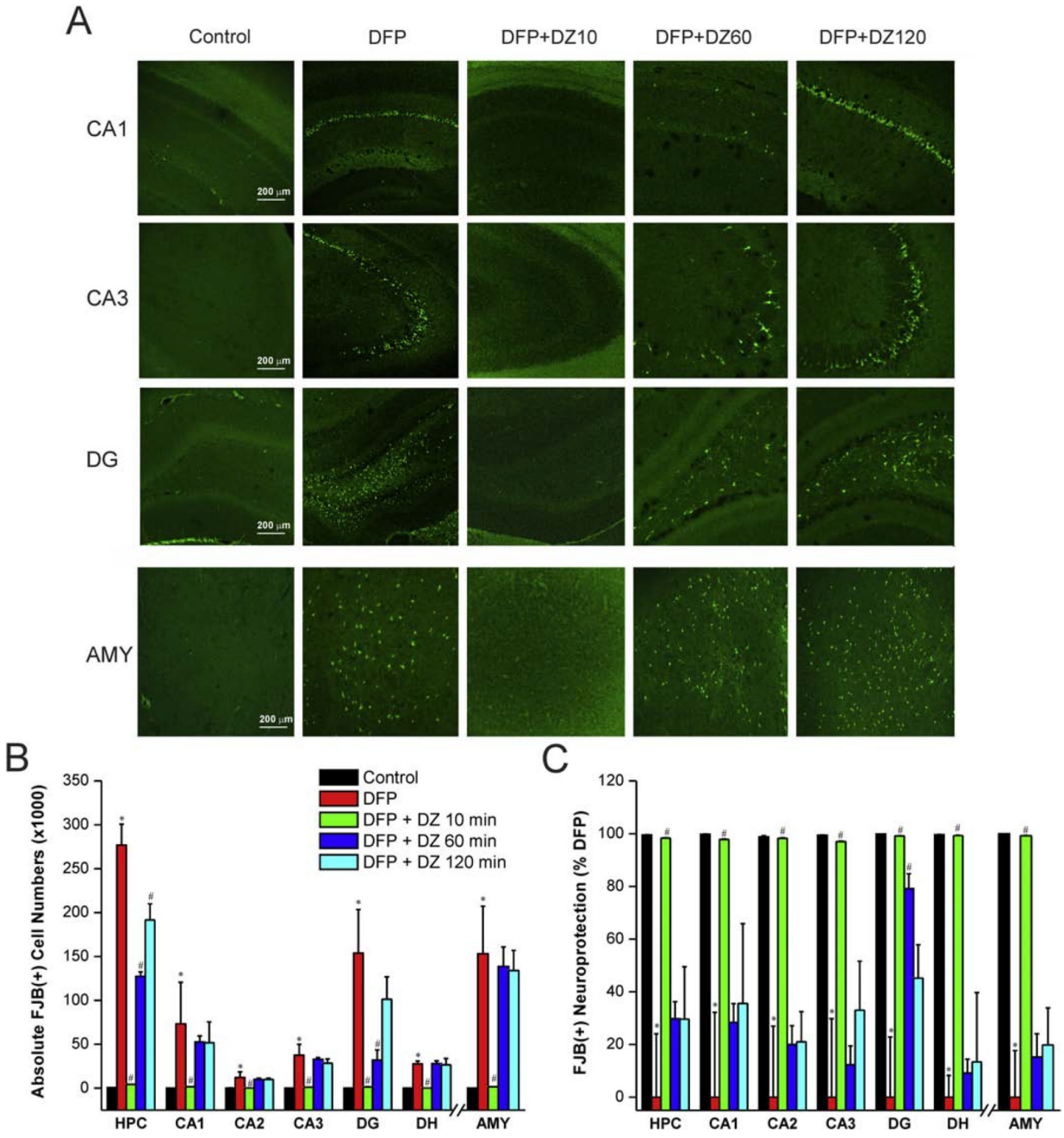

Fig. 5. Time-course profile of diazepam (5 mg/kg, IM) on DFP-induced FJB(+) neuronal injury and necrosis in the hippocampus (HPC) subfields and amygdala (AMY)

(A) FJB(+) staining depicting neurodegeneration in groups with or without diazepam treatment at 10 to 120 min post-DFP. (B) FJB(+) neuronal counts by stereology in hippocampus subfields and amygdala. (C) Normalized percent neuroprotection by diazepam at various time points after DFP. Value represent the mean ± SEM (n=4–6 rats per group). *p<0.05 vs control (no DFP); #p<0.05 vs DFP group (ANOVA and post hoc unpaired student *t*-test).

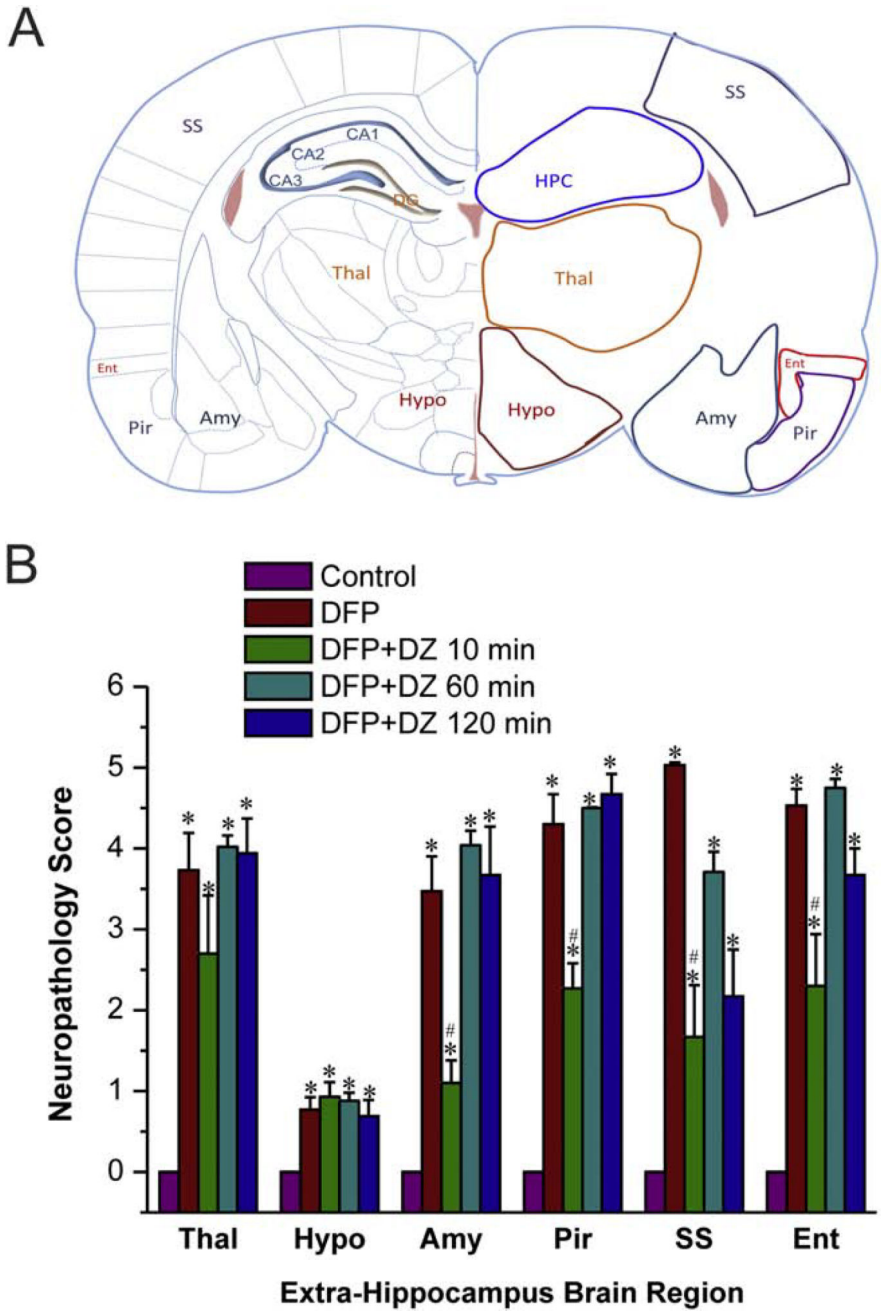

Fig. 6. Time-course profile of diazepam (5 mg/kg, IM) on DFP-induced FJB(+) neuronal injury and necrosis in the extrahippocampal regions

(A) Schematic illustration of brain regions selected for analysis of FJB(+) staining, including hippocampus (Hippo), thalamus (Thal), hypothalamus (Hypo), amygdala (Amy), pirform cortex (Pir) somatosensory cortex (SS), and entorhinal cortex (Ent) regions. (B) The bar charts depict neuropathology score results in the extra-hippocampus subfields. DFP induced SE resulted a high score (severe damage). Value bars represent the mean ± SEM (n=4–6 rats). Values represent the mean ± SEM (n=4–8 rats). *p<0.05 vs control (no DFP); #p<0.05 vs DFP group (ANOVA and post hoc unpaired student *t*-test).

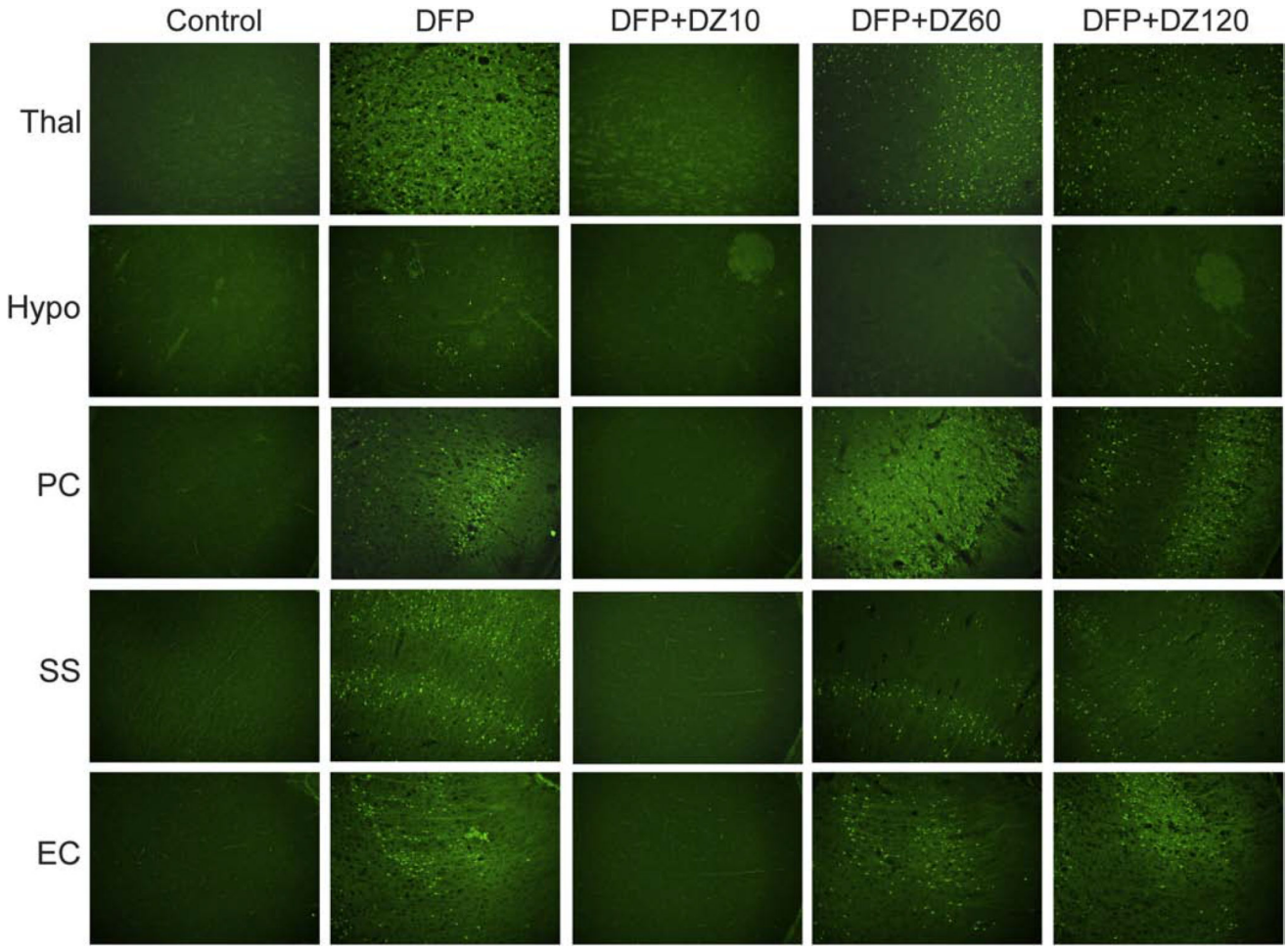

Fig. 7. Representative sections illustrating the effect of diazepam (5 mg/kg, IM) on DFP-induced FJB(+) neuronal injury and necrosis in the extrahippocampal regions

Brain regions selected for analysis of FJB(+) staining consist of thalamus (Thal), hypothalamus (Hypo), pirform cortex (Pir) somatosensory cortex (SS), and entorhinal cortex (Ent) regions.

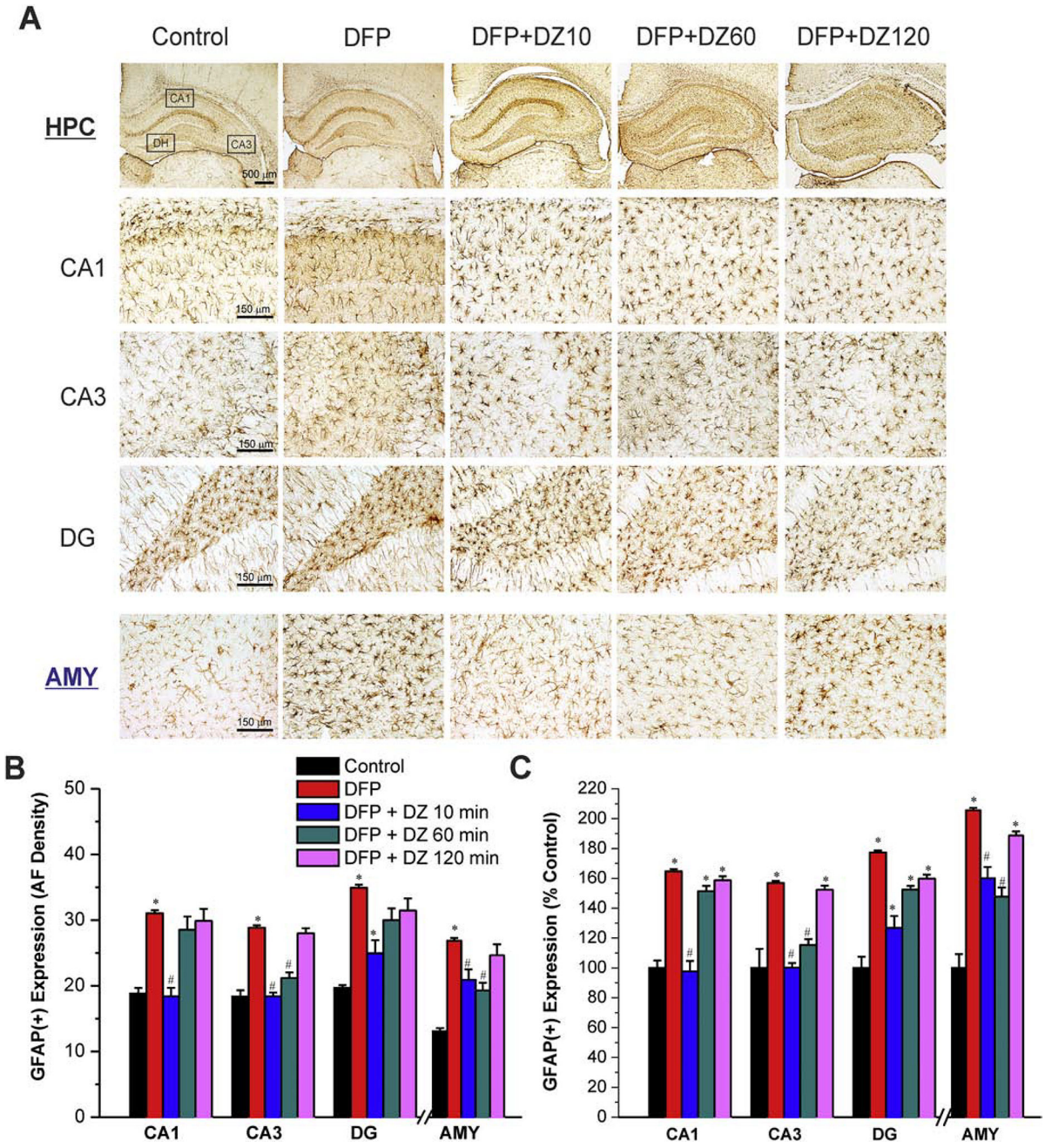

Fig. 8. Time-course profile of diazepam (5 mg/kg, IM) on DFP-induced GFAP(+) astrocyte activation and neuroinflammation in the hippocampus (HPC) and amygdala (AMY) regions

(A) Representative sections of GFAP(+) immunostaining in the hippocampus and amygdala. (B) The bar graph depict area fractionation densitometry quantification of GFAP(+) expression in the hippocampus subfields and amygdala. (C) Percent change in GFAP(+) expression in various subgroups in the hippocampus subfields and amygdala. Values represent the mean ± SEM (n=4–8 rats). *p<0.05 vs control (no DFP); #p<0.05 vs DFP group (ANOVA and post hoc unpaired student *t*-test).

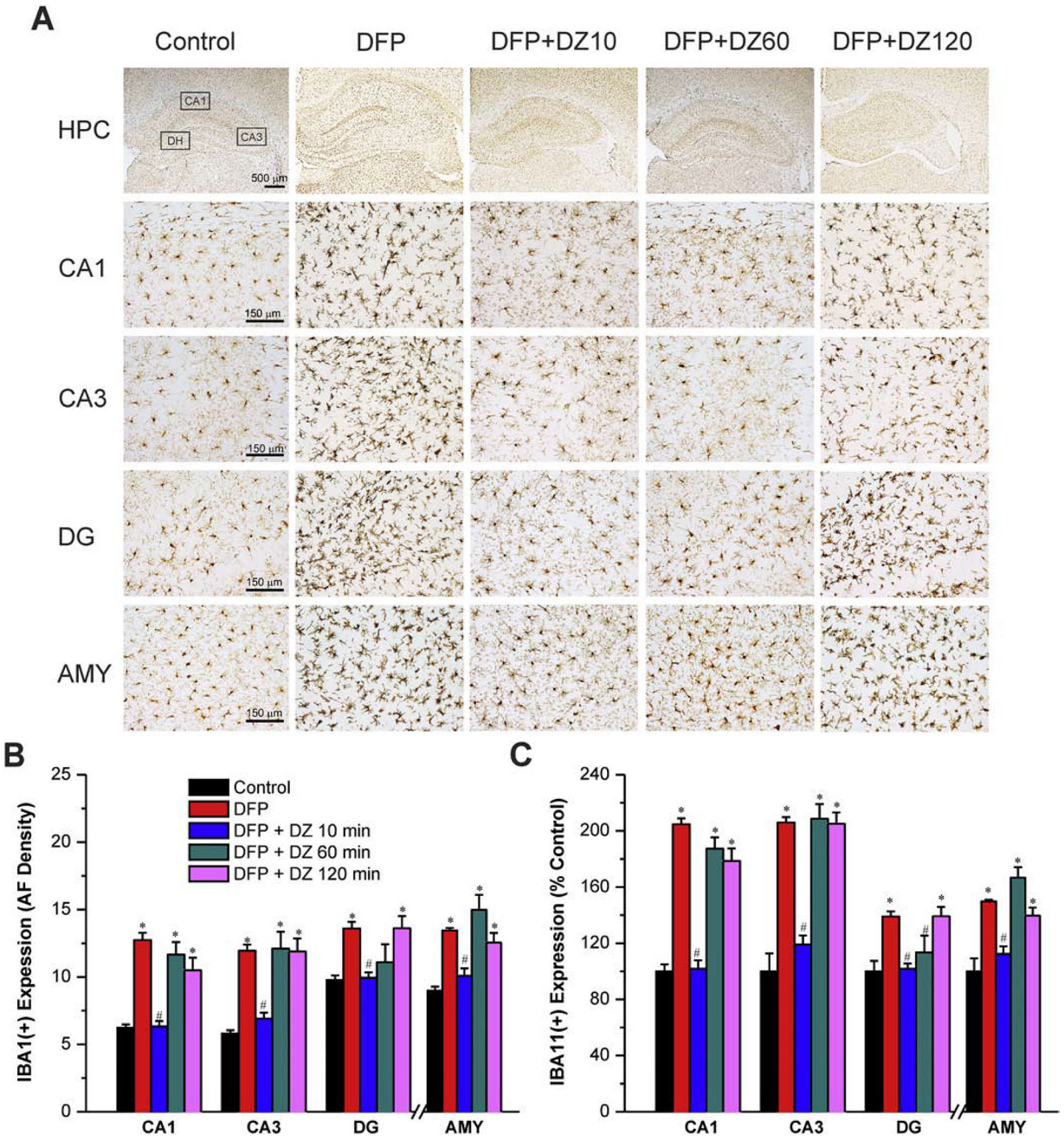

Fig. 9. Time-course profile of diazepam (5 mg/kg, IM) on DFP-induced IBA1(+) microglia activation and neuroinflammation in the hippocampus (HPC) and amygdala (AMY) regions

(A) Representative sections of IBA1(+) immunostaining in the hippocampus and amygdala. (B) The bar graph depict area fractionation densitometry quantification of IBA1(+) expression in the hippocampus subfields and amygdala. (C) Percent change in IBA1(+) expression in various subgroups in the hippocampus subfields and amygdala. Values represent the mean ± SEM (n=4–8 rats per group). *p<0.05 vs control (no DFP); #p<0.05 vs DFP group (ANOVA and post hoc unpaired student *t*-test).

Table 1

Summary time-course profile of diazepam (5 mg/kg, IM) therapy in the DFP model.

	Control	Diazepam		
Parameters		***10 min***	***60 min***	***120 min***
Number of rats	8	7	14	8
SE termination	0 (0%)	7 (100%)	1 (7%)	0 (0%)
Latency for SE termination	NA	~30 min	NT	NT
24 h Lethality	4 (50%)	0 (0%)	3 (21%)	2 (25%)

NA, not applicable; NT, termination was not observed